Bulgarian Chemical Communications, Volume 47, Special Issue D (pp. 233 - 240) 2015

A parametric study on the factors affecting gas turbine combustion using a CFD-based approach

Farhud Shirinzadeh[1], Reza Mohajer Barough[2], Ali Atashbar Orang[3*]

[1]*Department of Mechanical Engineering, Science and Research Branch, Islamic Azad University, Tehran, Iran*

[2]*Faculty of Mechanical Engineering, University of Tabriz, Tabriz, Iran*

[3]*Young Researchers and Elite Club, Tabriz Branch, Islamic Azad University, Tabriz, Iran*

Received June 26, 2015; Revised September 10, 2015

Abstract: In this paper, a numerical simulation was conducted using FLUENT CFD package to investigate injection effects of axial and swirl flow inside the annular combustion chamber with wall jet. The flow was considered as three-dimensional, steady, turbulent, incompressible, viscid, and two-phase and turbulence models including RNG (k-ε) and the Reynolds stress model were applied. In order to evaluate the applied numerical method, the results obtained in the reacting combustion chamber were compared with experimental ones. The effects of different parameters inside the combustion chamber including air-fuel ratio, swirl mass flow rate, fuel spray angle and swirl number were studied and optimal values for some of these values were obtained. The results showed that increasing the swirl air flow rate in the inlet area of the combustion chamber stretches the swirl area toward the fuel injection nozzles and causes initiation of combustion near the chamber inlet. The increase of the air-fuel ratio results in increasing the velocities and uniform temperature profiles in the outlet chamber. Increasing swirl number and decreasing fuel spray angle also reduces wall temperature. Optimal values for Sauter mean diameter and fuel spray angle were also determined.

Keywords: gas turbine combustion chamber; air-fuel ratio; fuel spray angle; swirl number

1. INTRODUCTION

Gas turbine combustion chambers need high combustion efficiency, low pollutants emissions and high performance. Turbulent flow field inside the combustion chamber plays a very important role in flame formation. Another important factor is the way in which fuel is injected into the combustion chamber and its mixing with air. Swirl flow has been mostly used to stabilize the flame inside the combustion chamber of gas turbines. Combustion modeling has a fundamental role in accurate simulation of combustion flows. This is, in addition to the amount of species and combustion products, energy release rate resulting from the mixing of the fuel and oxidant is determined by it. An appropriate combustion model should take into account the effect of all these factors. In computational fluid dynamics (CFD), the simulation of processes such as turbulence, combustion and radiation requires mathematical modeling. Simulation of these phenomena can be useful and reliable if the infrastructure model or models are accurate enough. The extensive applicability, high accuracy, low computational cost and simplicity are four important specifications of mathematical models.

Cameron and Samuelsen [1] studied the characteristics of temperature and velocity profiles inside a combustion chamber with wall jet. The obtained results indicated that velocity and temperature profiles are at isothermal and reactive conditions, respectively. They also investigated the effect of swirl air increasing and fuel droplet atomization. Sue et al. [2] investigated numerically a gas turbine chamber integrated with the diffuser. They used the KIVA-3V code to analyze the flow inside the combustion chamber. Flow fields and temperature distribution were studied along the axial and circumferential directions and the stable behavior of the flow in the combustion-compressor system was evaluated. Zhang et al. [3] studied the thermodynamic conditions inside a combustion chamber considered to be symmetric and two-dimensional. The effects of equivalence ratio, reaction temperature and swirl inside the cylindrical combustion chamber were investigated. The results obtained indicated that the combustion chamber geometry has a trivial effect on pressure fluctuation inside it. Som et al. [4] studied the effect of inlet air swirl and fuel injection angle inside a gas turbine

To whom all correspondence should be sent:
E-mail: Ali.at.orang@gmail.com

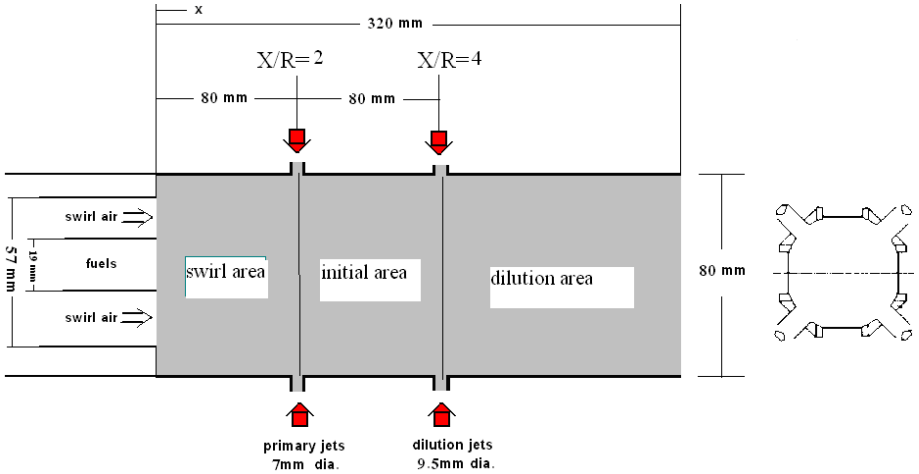

Fig. 1. Schematic of combustion chamber wall jet model

combustion chamber. The results revealed that unlike low swirl numbers, a spiral swirl zone could be seen around the initial central zone at a high swirl numbers. Kurosavwa et al. [5] studied the swirl flame structure inside a gas turbine combustion chamber. They focused on high combustion efficiency, low emissions inside the combustion chamber. Olivani et al. [6] investigated the structure of reactive and non-reactive swirl flows. They found that although the overall mixing process and the main flame structure were handled by the air flow swirl, the fuel injection methods have an important effect on them at the initial zone. Sandararaj et al. [7] studied the effects of jet injection angle, cross-flow Reynolds number and velocity ratio on entrainment and mixing of jet with incompressible cross-flow in venturi-jet mixer.

This paper deals with the effects of axial and swirl air injection and the determination of optimal values for effective parameters including swirl air flow rate, expansion angle of inlet air, diameter of the initial fuel droplets and fuel spray angle. The results of this work can be used for the preliminary design of the aircraft gas turbine combustion chambers and liquid fuel missiles. Furthermore, the optimal values obtained for the average diameter of primary particles and fuel spray angle can be used in design procedures.

2. GEOMETRICAL MODEL AND NUMERICAL METHOD

The wall jet model acts at atmospheric pressure with JP4 fuel. Combustion chamber air is preheated to 600 °C and air flow rate is 163 kg/h. Fuel flow rate and the temperature are 3.27 kg/h and 400 °C, respectively, for an equivalence ratio of 0.3. As shown in Figure 1, air flow is divided into swirl jet, initial jet and diluted air jet. The longitudinal four valves are built around the chamber. Initial jets and diluted air jets have diameter of 7 mm and 9.5 mm, respectively. A stainless steel channel with radius of 40 cm and length of 32 cm is considered which is blocked from 57 mm onwards. A 60 degree turning is built in the inlet chamber. One of the main needs of gas turbine combustion chambers is that the combustion chamber operates at every working condition. The flow pattern is the first factor of the chamber that affects flame stability. The most common method is recirculation of part of combustion products to the upstream flow and remixing of products with fuel and fresh air. One conventional method involves the use of swirl to create a recirculation. In this design, air nozzles surround the fuel injectors which increase the shear stress and turbulence intensity inside the chamber.

The combustion chamber mesh has been built in GAMBIT as shown in Figure 2. It is a 100×80×40 mesh along r,θ,z directions. The FLUNET 6.3 package is used for the simulations. A segregated solver is used to solve the governing equations and an implicit form is used for the linearization of the equations. Convective and diffusion terms are discretized based on power-law and central schemes, respectively. Pressure and velocity fields are coupled through the simple algorithm and Eddy dissipation model is used to model the interactions among them.

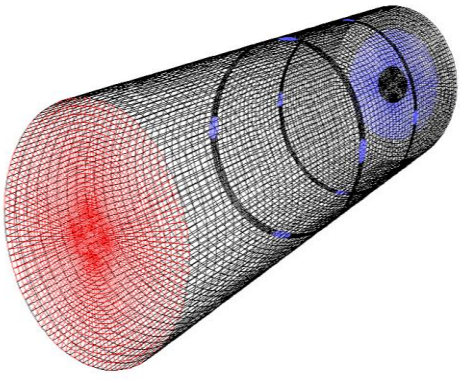

Fig. 2. Combustion chamber mesh

3. GOVERNING EQUATIONS

The Navier-Stokes equations are the fundamental partial-differential equations that describe the flow of fluids. Mass conservation equation or continuity equation, is written as following,

$$\frac{\partial \rho}{\partial t} + \frac{\partial}{\partial X_i}(\rho U_i) = S_m \tag{1}$$

- Momentum conservation equations,

$$\frac{\partial}{\partial t}(\rho U_i) + \frac{\partial}{\partial X_j}(\rho U_i U_J) = -\frac{\partial p}{\partial X_i} + \frac{\partial \tau_{ij}}{\partial X_j} + \rho g_i + \dot{S}_{M_i} \tag{2}$$

- Kinetic energy of turbulence,

$$\rho \frac{Dk}{Dt} = \frac{\partial}{\partial x_i}\left[\left(\mu + \frac{\mu_t}{\sigma_k}\right)\frac{\partial k}{\partial x_i}\right] + G_K + G_b - \rho\varepsilon - Y_m \tag{3}$$

- Dissipation rate of turbulent kinetic energy,

$$\rho \frac{D\varepsilon}{Dt} = \frac{\partial}{\partial x_i}\left[\left(\mu + \frac{\mu_t}{\sigma_\varepsilon}\right)\frac{\partial \varepsilon}{\partial x_i}\right] + C_{1\varepsilon}\frac{\varepsilon}{K}(G_k + C_{3\varepsilon}G_b) - C_{2\varepsilon}\rho\frac{\varepsilon^2}{k} \tag{4}$$

- Energy equation,

$$\frac{\partial}{\partial t}(\rho^g c_p^g T) + \frac{\partial}{\partial x_i}(\rho^g c_p^g U_i T) = \frac{\partial}{\partial x_i}(\rho^g c_p^g \alpha_{eff}\frac{\partial T}{\partial x_i}) - \frac{\partial q_i^r}{\partial x_i} + \overset{*}{S}_E \tag{5}$$

- Discrete phase model: Fuel spray (continuous injection in the combustion chamber), includes a limited number of droplet categories with a range of specific sizes. Initial droplet size distribution of liquid fuel spray is assumed to follow Rosin-Rammler distribution function defined as,

$$G'(d_i) = \frac{\exp(-bd_i^n) - \exp(-bd_{\max_i}^n)}{\exp(-bd_{\min_i}^n) - \exp(-bd_{\max_i}^n)} \tag{6}$$

- Species conservation equation,

$$\frac{\partial}{\partial t}(\rho^g C_j) + \frac{\partial}{\partial x_i}(\rho^g U_I C_j) = \frac{\partial}{\partial x_i}(\rho^g D_{eff}\frac{\partial C_j}{\partial x_i}) + \dot{S}_{C_j} + \dot{S}C_j \tag{7}$$

- Eddy dissipation model is,

$$\overline{\omega_P} = \rho C_{EBU}\frac{\varepsilon}{K}\left(\overline{Y_P''^2}\right)^{\frac{1}{2}} \tag{8}$$

The dimensionless number swirl used to determine the swirl applied on the flow, is defined as:

$$S_N = \frac{2G_m}{D_{SW}G_t} \tag{9}$$

where G_m, G_t and D_{sw} are axial flux of angular momentum, axial flux of axial momentum and swirl outer diameter, respectively. These parameters are given in turn by,

$$G_t = \int_0^{\frac{D_{sw}}{2}} 2\pi r\rho U(U)dr + \int_0^{\frac{D_{sw}}{2}} 2\pi r P dr \tag{10}$$

$$G_m = \int_0^{\frac{D_{sw}}{2}} 2\pi r\rho U(Wr)dr \tag{11}$$

where *W*, *U* and *P* are axial velocity, tangential velocity and static pressure, respectively. There is usually no reverse flow for $S_N < 0.4$. The stream lines show considerable divergence for $0.4 < S_N < 0.6$. Reverse flow was observed for $S_N > 0.6$. The following relation is proposed for calculating the swirl number in one-axial swirl with flat blades,

$$S_n = \frac{2}{3}\frac{1-(\frac{D_{hub}}{D_{sw}})^3}{1-(\frac{D_{hub}}{D_{sw}})^2}\tan(\theta) \tag{12}$$

where the model factor is defined as,

$$P.F = \frac{T_{\max} - T_{av}}{T_{av} - T_{in}} \tag{13}$$

here T_{max}, T_{av} and T_{in} are the maximum temperature at the outlet section, weighted average temperature in chamber outlet, and weighted average temperature of all chamber inlets, respectively.

4. RESULTS AND DISCUSSION

Referring to Figure 1, swirl air inlet, initial jets and dilution jets are considered as 25, 35 and 40 percent of the total air flow rate, respectively [1]. The results obtained show that the onset of swirl area is in the trap area at X/R=0.75 in reactive condition. Figures 3 and 4 illustrate the axial velocity and temperature profiles in different cross-sections, respectively. In order to detect the effects of initial jets on the swirl area, $x/R = 1$ has been used. Regarding the total inlet air, 50% for swirl air, 50% for diluted air and 0% for the primary air is utilized. According to Figure 5, temperature is initially high across the swirl area except near the wall because the combustion occurs at this region. Temperature in the downstream of flow is decreased due to increased

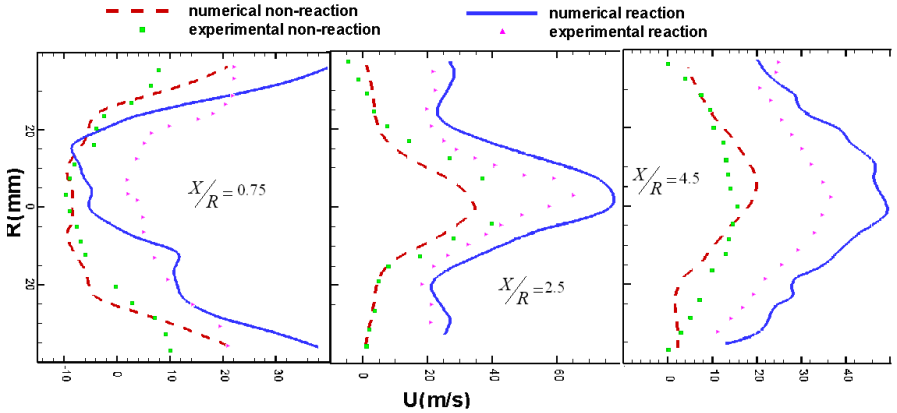

Fig. 3. Axial velocity comparison with reactive and isothermal conditions (Re=19600, S=0.36, A/F=1.5)

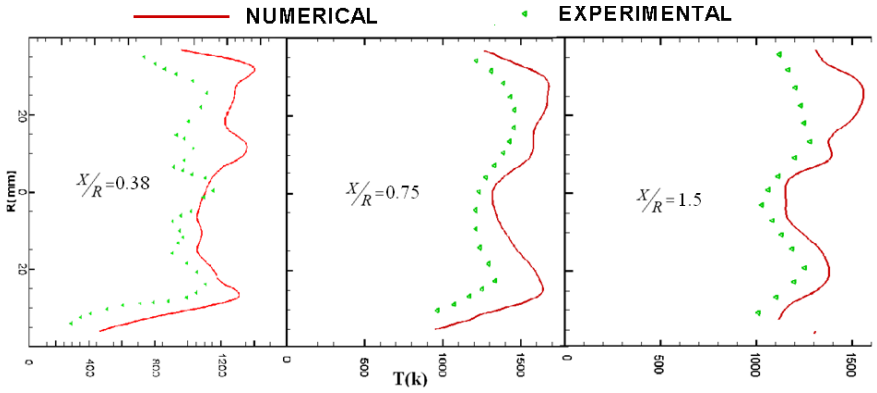

Fig. 4. Total temperature profiles in reactive condition at trap zone (Re=19600, S=0.36, A/F=1.5)

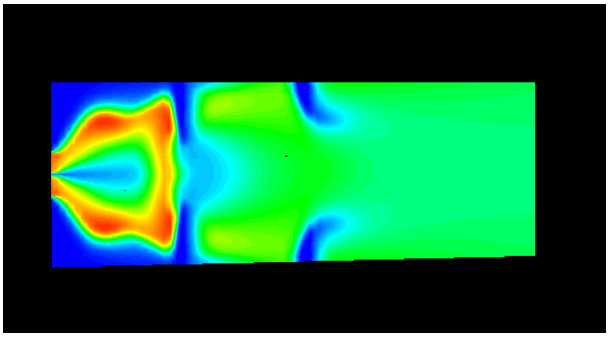

Fig. 5. Temperature profile at reaction case

penetration of the jets and extreme enhancement of the axial velocity in the central line. At outer areas of the combustion chamber due to the penetration of diluted jets, the temperature profile is relatively uniform. Figure 6 shows the variation of radial velocity in the case of swirl air enhancement. A 45 degree expansion is gradually influencing the progress of the swirl flow. The reason for this is that a mechanism was added to the swirl created in the trap area which affected the reverse mixture and, as can be seen in Figure 7, the swirl occurred at $x/R =$ 0.63.

The effect of increasing the fuel-air ratio from 1.5 to 3 on the axial velocity and temperature profiles is shown in Figures 8 and 9, respectively. This effect is mostly evident in the trap area at $x/R =$ 0.38, 0.75 and 1.13. Although, the velocity profiles are similar to those obtained in the previous air-fuel ratio (A/F=1.5), velocities become much larger. The effect of increasing air-fuel ratio is gradually reduced at $x/R = 2.5$ and 4.5. Asymmetry in the temperature profiles near the nozzle at $x/R =$ 0.38 is again evident. Although the hot strip exists in these conditions, its effect is much less. Temperature profiles are relatively symmetric about the central line. The cool core resulting from the jets penetration appears at $x/R = 2.5$ and continues through the flow up to $x/R = 4.5$. The temperature profile is relatively uniform at $x/R = 5$.

The effects of swirl number on the chamber wall temperature and output temperature are shown in Figures 10 and 11, respectively.

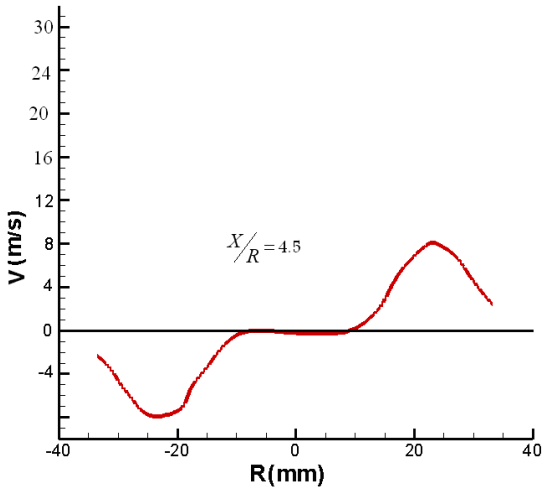

Fig. 6. Variation of radial velocity with swirl air enhancement.

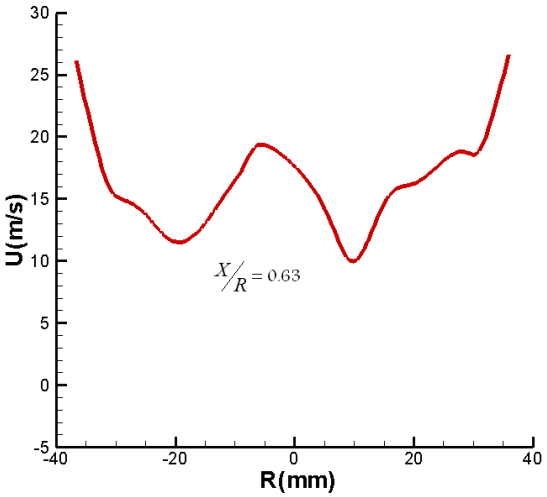

Fig. 7. Velocity profile in the case of 45^0 gradual increasing.

According to Figure 10, the slope of the curve in trap area is caused by chemical interactions. The wall temperature rapidly decreased due to the primary air jet entering to the chamber, and then, because of heat penetration from the core, the temperature near the wall relatively increases. Then, a large drop in wall temperature occurs due to the entering of diluted air followed by an increase in wall temperature up to the outlet. By increasing the swirl number through the increase of the swirl angle, the combustion is prevented from reaching the walls and, as depicted in Figure 13 the temperature near the wall falls. As can be seen in Figure 11, by increasing the swirl number, the outlet temperature reduces near the wall and increases in the central line. The reason for this is that by increasing the swirl number more combustion occurs on the central line and it is not drawn near the wall.

According to Figure 12, by increasing the fuel spray angle, the wall temperature increases due to large radial dispersion of fuel particles and subsequent combustion of the fuel near the wall.

Outlet temperature variation based on the fuel spray angle is shown in Figure 13. As observed in Figure 13, by increasing the angle of fuel spray, the fuel mixes better with air and most of the reaction process is occurs in the trap area, consequently, the outlet temperature falls.

For issues related to gas turbine combustion, small Sauter mean diameter of the initial fuel droplets increases efficiency and engine performance and reduce pollutants; on the other hand, if the droplet size is too small, they lose the required momentum and force to penetrate into high-pressure gases. Figure 14 depicts the Sauter mean diameter of initial droplets with a constant spray angle of 80^0. Combustion efficiency, and P.F. are calculated for several Sauter mean diameters. The mean diameter of initial droplets of 52 μm has more suitable combustion efficiency and P.F. compared to other diameters. As can be seen in Figure 15, the spray angle of 80^0 results in the highest combustion efficiency and P.F. According to experimental results available in literature, P.F. is between 0.5 and 0.75 [8].

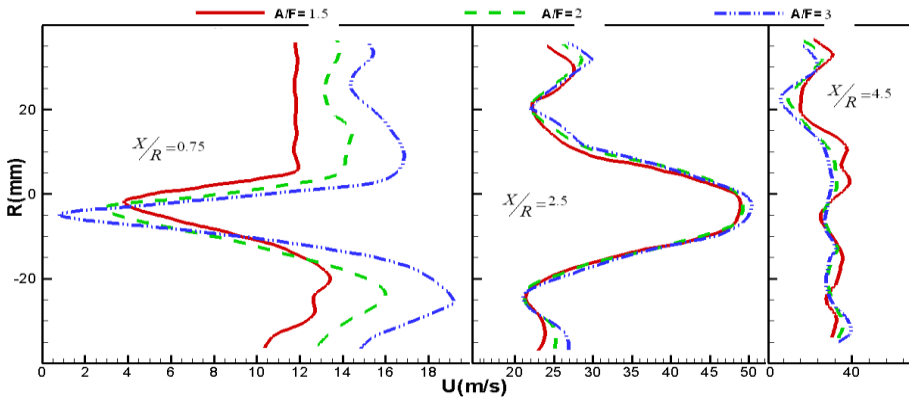

Fig. 8. Axial velocity profiles at three different air-fuel ratios.

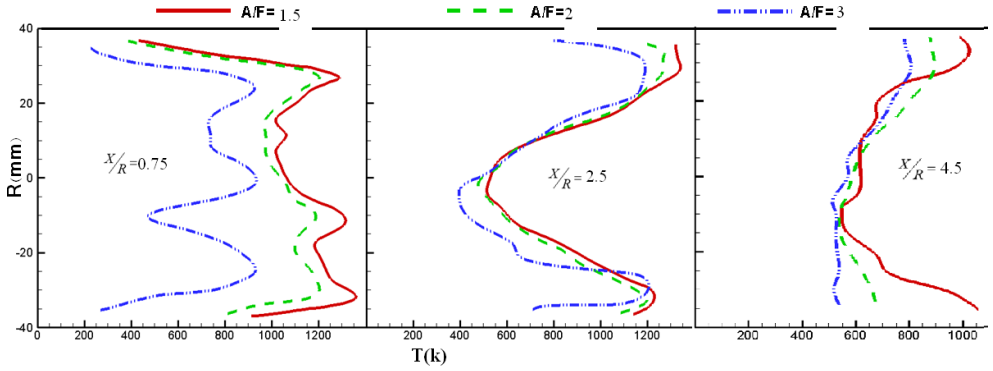

Fig. 9. Temperature profiles at three different air-fuel ratios.

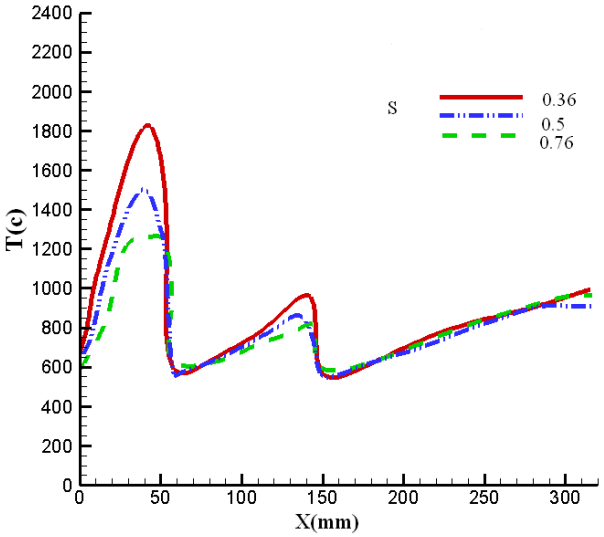

Fig. 10. Effect of swirl number in different cases of wall temperature.

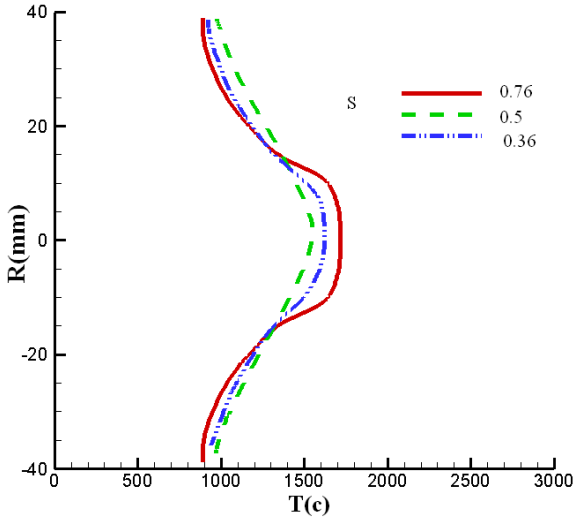

Fig. 11. Effect of swirl number in different cases of outlet temperature.

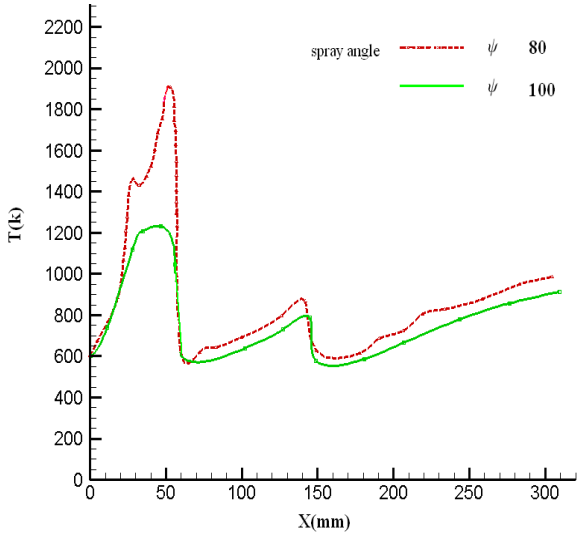

Fig. 12. Effect of fuel spray angle on wall temperature.

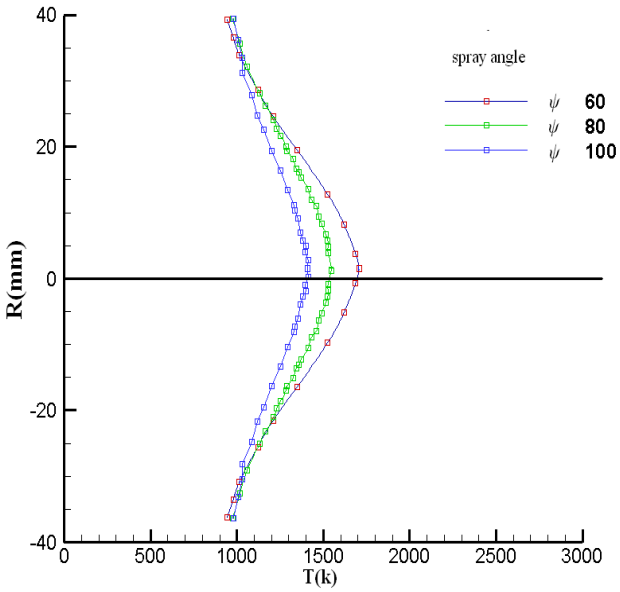

Fig. 13. Effect of fuel spray angle on outlet temperature.

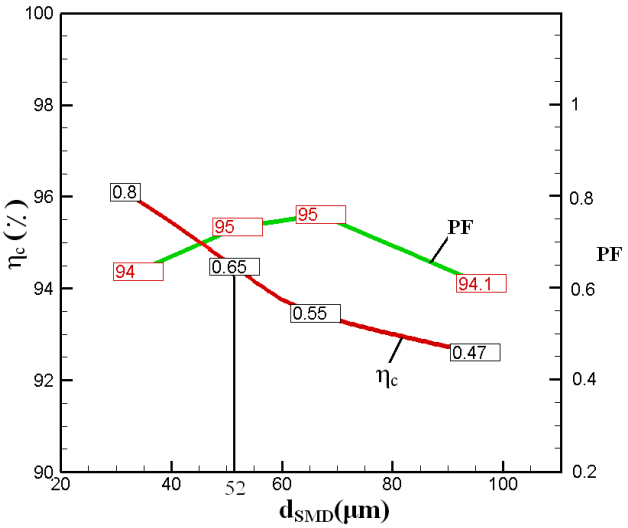

Fig. 14. Optimization of Sauter mean diameter of initial droplets.

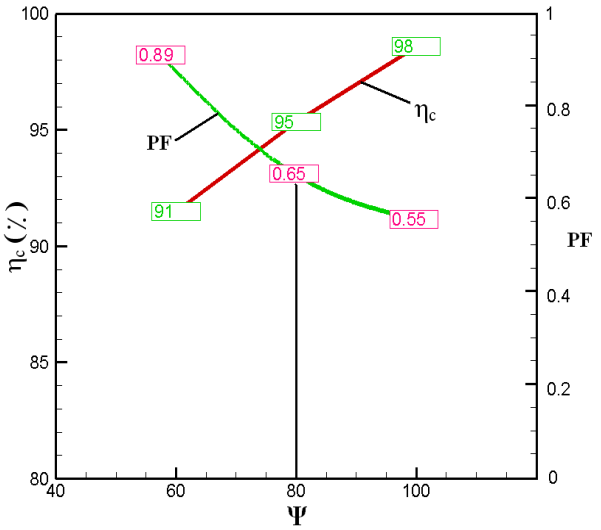

Fig. 15. Optimization of fuel spray angle.

5. CONCLUSIONS

A numerical simulation was performed to investigate the effects of injection of axial and swirl flow inside an annular combustion chamber with wall jet. According to the results, by increasing the flow rate of swirl air entering the combustion chamber it is possible to achieve a rapid and nearly complete mixing mode. An excessive increase in the swirl flow rate at the chamber inlet allows that the combustion reaches the fuel injection nozzles. Thus, an optimum value for the swirl air flow exists. The effect of swirl number and fuel spray angle on wall and outlet temperatures were also investigated. Increasing the swirl air flow rate in the inlet area of the combustion chamber stretches the rotational area toward the fuel injection nozzles and causes the initiation of combustion near the chamber inlet. A further increase of the swirl flow rate at the chamber entrance makes that the combustion reaches the fuel injection nozzle; hence, an optimal value for swirl flow rate in the chamber entrance needs to be determined. An increase in the air-fuel ratio results in an increase in the velocities and uniform temperature profiles at the outlet chamber. Moreover, increasing swirl number and decreasing fuel spray angle also reduces the wall temperature. According to the results obtained, by enhancing the inlet swirl air flow rate and a sudden 45^0 expansion through variation in the geometry of the combustion chamber, rapid and quite complete mixing can be achieved. However, due to the proximity of the combustion to the chamber inlet and subsequent damage of the fuel injection nozzle, optimal values need to be obtained for the mentioned parameters.

NOMENCLATURE

S_m	Mass added to the continuous phase of the second diffused phase
p	Static pressure
τ_{ij}	Stress tensor
ρg_i	Gravitational force along i direction
$\dot{S}_{M_i}$	Momentum term in gas phase equation
G_K	Turbulent kinetic energy
G_b	Kinetic energy of buoyancy
Y_m	Fluctuating expansion in compressible Turbulence relative to the overall loss rate
σ_k	Turbulent Prantl number
σ_ε	Turbulent Prantl number
$\dot{S}_E$	energy term
$\dot{G}(d_i)$	Mass fraction of spray
$\overset{*}{S}_{Cj}$	Source term
$\overline{Y_P''^2}$	Variance of product mass fraction

REFERENCES

1. C.D. Cameron, G.S. Samuelsen, *ASME J. Eng. Gas Turbine Power*, **111**, 31 (1989).
2. K. Su, C.Q., Zhou Numerical Modeling of Gas Turbine Combustor Integrated with Diffuser.34th National Heat Transfer conference Pittsburgh, 2000.
3. C. Zhang, T. Zhao, Parametric Effects on Combustion Instability in a Lean Premixed Dump Combustor. AIAA-02-4014, 2005.

4. S.K. Som, A.K. Ghosh, Effects of Inlet Air Swirl and Spray Cone Angle on Combustion and Emission Performance of a Liquid Fuel Spray in a Gas Turbine Combustor. Dissertation, Wright-Patterson Air Force Base, Dayton, Ohio, July 2000.
5. Y. Kurosavwa, S. Yoshida, T. Yamamoto, K. Shiodira, M. Gomi, K. Suzuki, Structure of Swirler in Gas Turbine Combustor.Technical Report National Aerospace Laboratory of Japan, 2000.
6. A. Olivani, G. Solero, F. Cozzi, A. Coghe, *Exper. Thermal Fluid Sci.*, **31**, 427 (2007).
7. S. Sandararaj, V. Selladurai, *Thermal Sci.*, **16**, 207 (2012).
8. X.R. Duan, W. Meirer, P. Weigand, B.Lehmann, *Lasers and Optics*, **127**, 492 (2005).